Non-invasive low charge electron beam time-of-arrival diagnostic using a plasmonics-enhanced photoconductive antenna

E. C. Snively,[1,a)] N. T. Yardimci,[2] B. T. Jacobson,[3,b)] M. Jarrahi,[2] P. Musumeci,[1] and A. Murokh[3]
[1]*Department of Physics and Astronomy, UCLA, Los Angeles, California 90095, USA*
[2]*Department of Electrical and Computer Engineering, UCLA, Los Angeles, California 90095, USA*
[3]*RadiaBeam Technologies, Santa Monica, California 90405, USA*

(Received 20 August 2018; accepted 22 October 2018; published online 5 November 2018)

The use of a plasmonics-enhanced photoconductive antenna (PCA) optically gated by a near infrared (NIR) pulse enables non-invasive time-of-arrival measurements of a low charge electron beam with respect to the NIR reference, achieving picosecond resolution. The measured signal values show the expected scaling with the beam charge and distance from PCA to the beam axis, as the PCA samples the electric field of the passing electron beam. We operate the device with an NIR spot size much larger than the PCA active-area, resulting in a very simple optical setup and alignment procedure, making the plasmonics-enhanced PCA a preferred alternative to more complex timing diagnostics for applications requiring non-invasive picosecond or sub-picosecond time-stamping. © *2018 Author(s). All article content, except where otherwise noted, is licensed under a Creative Commons Attribution (CC BY) license (http://creativecommons.org/licenses/by/4.0/).*
https://doi.org/10.1063/1.5052631

Rapid progress in nanofabrication techniques has allowed breakthrough advances in our ability to control electromagnetic fields in space and time at the sub-wavelength scale, revolutionizing many research areas. Among these, the introduction of nanoscale devices in particle accelerators has the potential to solve some of the outstanding challenges in conventional techniques. Some recent examples, restricting the discussion to metal-based nanostructures, include the use of plasmonics-based devices for electron beam generation[1] and acceleration.[2]

Demand is growing within the accelerator field for precise synchronization and non-invasive monitoring of the relative time-of-arrival of a charged particle beam with an external reference laser pulse. Time-of-arrival diagnostics are in fact critical for all advanced accelerator applications which require the simultaneous use of an ultrafast laser pulse and a relativistic electron beam, including ultrafast electron diffraction (UED),[3–5] X-ray free electron lasers,[6–8] inverse Compton scattering sources,[9] and beam and laser driven plasma wakefield acceleration schemes.[10,11] Due to the limits in the stability of accelerator drive sources, a significant jitter (of order tens to hundreds of fs, depending on the size and scale of the machine) in the timing of electron beams is unavoidable[12–15] and accurate timestamping of an electron beam is essential in post-processing of time-dependent results in pump-probe experiments.[16] Non-invasive timing diagnostics can also provide feedback for time-of-arrival stabilization for short wavelength laser-driven accelerator sections.[17,18]

Button and stripline beam position monitors as well as RF cavity based detection schemes are the traditional solutions in the accelerator field for this application and can achieve timing resolution with sub-10 fs precision but require integration over many beam shots and large bunch charges (hundreds of pC).[19–22] Electro-optic sampling techniques have also been employed and demonstrated single-shot time-of-arrival resolution down to the 10 fs level[10,17,23,24] but require challengingly precise alignment with multiple optical components and are only feasible when the beam charge is greater than 10 pC.

In this paper, we discuss the use of a plasmonics-enhanced photoconductive antenna (PCA) initially developed for terahertz emission and detection[25,26] for a robust non-invasive beam timing diagnostic of low charge relativistic electron beams. Unlike previous studies using a PCA for coherent detection of the transient electric field from photoconductive or nonlinear radiation sources[27–29] or the coherent transition radiation from an electron beam,[30,31] the increased sensitivity due to the plasmonic enhancement allows measurements of the transient electric field of a sub-10 pC relativistic electron bunch passing close to the PCA. In our discussion, we elaborate on design improvements that could push the diagnostic technique to femtocoulomb sensitivity.

A PCA consists of a metallic antenna and a photoconductive semiconductor on which the antenna is deposited. These devices can be used commonly for both terahertz pulse generation and detection. A sub-picosecond optical pulse is used to optically excite the region between the antenna arms, generating a large carrier population in the photoconductor. For terahertz wave detection, the incident terahertz radiation on the PCA drives the generated photocurrent which is integrated by an unbiased transimpedance amplifier. Hence, the strength of the generated photocurrent is directly proportional to the incident terahertz field. Short-carrier lifetime photoconductors, such as low-temperature-grown GaAs (LT-GaAs), are usually used as the photo-absorbing substrate to ensure the ultrafast operation of PCAs.

[a)]Electronic mail: ejcurry@physics.ucla.edu
[b)]Present address: SLAC National Accelerator Laboratory, 2575 Sand Hill Road, Menlo Park, California 94025, USA.

 © Author(s) 2018.

A key feature of the PCA-based timing diagnostic is the capacity for the non-invasive measurement. The PCA is far enough from the electron beam axis that the beam can pass unobstructed and be used for further interactions or measurements. However, the electric field of the electron beam drops off quickly with the increasing radial distance from the beam center, see measurements in Fig. 5, so enhancements to detector sensitivity and responsivity are critical to performance. Plasmonics-enhanced PCAs have proven to be efficient tools to meet this criterion.[32,33]

The measurements presented here use a plasmonic photoconductive nanoantenna array fabricated over a large area (1 mm × 1 mm) on a LT-GaAs substrate.[25] The large area device captures a greater fraction of the total electric field compared to conventional PCAs and simplifies the alignment of the near infrared (NIR) beam by easing the need for tight focusing on the PCA active area. PCA detection benefits from operation with large area devices and NIR beams having large spot sizes, because the PCA output signal sums the contributions from all regions, enabling sensitivity to low-intensity THz fields. This feature provides a key advantage when comparing the technique to electro-optic detection.[34] The plasmonic nanoantennas are designed to offer extraordinary NIR transmission through the subwavelength gaps between them by the excitation of the surface plasmon waves at the NIR wavelength. Therefore, NIR absorption is enhanced significantly in close proximity to the nanoantennas. Because they are also designed to serve as broadband terahertz antennas, the nanoantennas maximize the interaction between the incident NIR pulse and the electric field of the relativistic electron bunch at the nanoscale. All nanoantenna arrays are connected together and shadow metal stripes are used to prevent the generation of photocurrents flowing in the opposite direction between the adjacent nanoantenna arrays that would reduce the total current through the device, see Fig. 1. A silicon nitride anti-reflection coating is used to further enhance the coupling of the NIR beam to the PCA.

Characterization of this PCA-based timing diagnostic is performed on the PEGASUS beamline at UCLA, see Table I for parameters. A Ti:sapphire laser is used to provide the NIR pulse for optically gating the PCA. The NIR pulse is also used to produce a UV pulse for driving the electron beam generation in a 1.6 cell S-band photogun, with an inherent timing synchronization to the NIR pulse. To monitor the electron beam position relative to the PCA, a phosphor screen is attached to the PCA mount and observed with a CCD camera. The assembly is then aligned with respect to the beam axis using a remotely controlled two-axis stage. The beam electric field points radially away from the electron beam axis and is localized in a disk perpendicular to the direction of electron motion, as shown in Fig. 2. Since the plasmonics-enhanced PCA is sensitive to the polarization of the radiation,[25] the device is aligned just below the beam axis in order to probe the vertical component of the beam electric field. The NIR pulse polarization is perpendicular to the nanoantennas, i.e., horizontal in the lab frame. To increase the NIR intensity on the PCA active area and thereby the photocarrier population which can respond to the excitation field, the NIR beam is focused by a lens 80 cm upstream. The NIR beam illuminates the PCA board at an angle of about 25° in order to keep the laser transport optics out of the path of the electron beam. In future optimized setups, this angle could be reduced to <5° to minimize any temporal broadening associated with the oblique incidence.

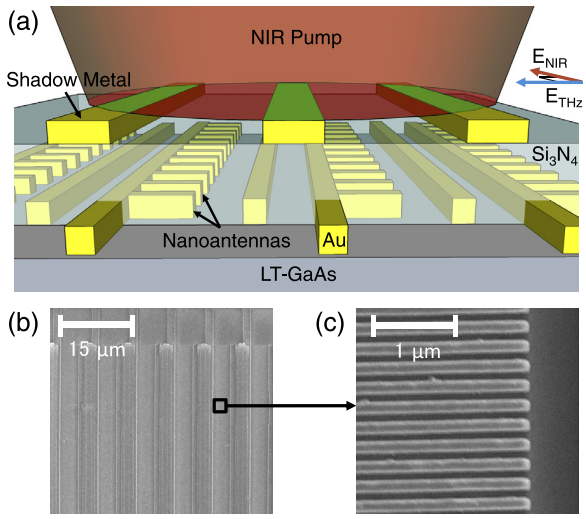

FIG. 1. (a) Schematic diagram of the plasmonics-enhanced photoconductive antenna (PCA) based on plasmonic nanoantenna arrays. The nanoantennas are deposited on low-temperature-grown GaAs (LT-GaAs). An antireflection coating is used to enhance NIR coupling to the photoconductor, and shadow metals are used to ensure that all the generated photocurrent components have the same polarity. The incident THz electric field must be polarized perpendicular to the shadow metals, as shown by the blue arrow; the NIR electric field should be polarized parallel to the shadow metals, as shown by the red arrow. Scanning electron microscopy (SEM) images of a fabricated plasmonics-enhanced PCA and the plasmonic nanoantennas are shown in (b) and (c), respectively.

The time-of-arrival scan shown in Fig. 3 uses a delay stage to adjust the path length of the NIR pulse, shifting the sub-picosecond time window in which photocarriers are generated in the PCA. When the NIR and electron beam arrival times are synchronized, radiation from the electron beam drives a current across the device, which is then converted to a voltage using a transimpedance amplifier with a gain of 10^7 and 500 kHz bandwidth (FEMTO Model No. DLPCA-200). Signal transport from the PCA in vacuum to the amplifier is accomplished with a triaxial feedthrough for enhanced shielding. The induced voltage is monitored using a sampling oscilloscope with a 50 Ω termination. The trace has a background level of 200 mV spanning several μs associated with the electromagnetic noise from the high power RF system driving the accelerator. The NIR pulse produces a 50 mV signal on top of this background.

To measure the electron beam-induced changes to the signal, we record the average of multiple oscilloscope traces, gated by a 1 μs window around the peak of the signal from

TABLE I. PEGASUS experimental parameters.

Electron beam energy	3.3 MeV
Bunch length (RMS)	1 ps
Charge	2–24 pC
Spot size	1 mm
Optical pulse wavelength	800 nm
Pulse duration	50 fs
Pulse energy	5 μJ

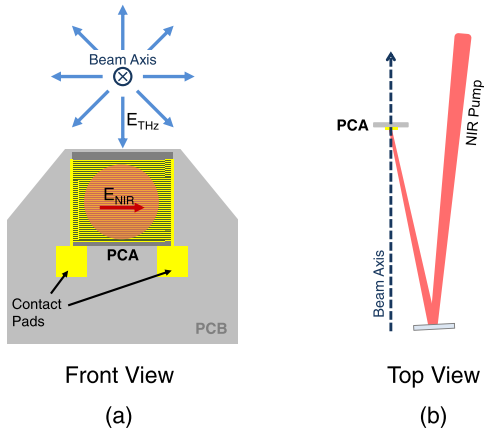

FIG. 2. (a) Diagram of the PCA mounted on a printed circuit board (PCB). The electron beam propagates above the board, into the page from this perspective, producing a radially polarized electric field. The NIR pulse that produces the photo-generated electrons and holes is shown by the red circle on the PCA active area, but the spot size can be even larger than the PCA area, without undermining the performance of the device. The NIR pulse is horizontally polarized, as shown by the red arrow. (b) View of the NIR path onto the PCA and the electron beam path above the PCA.

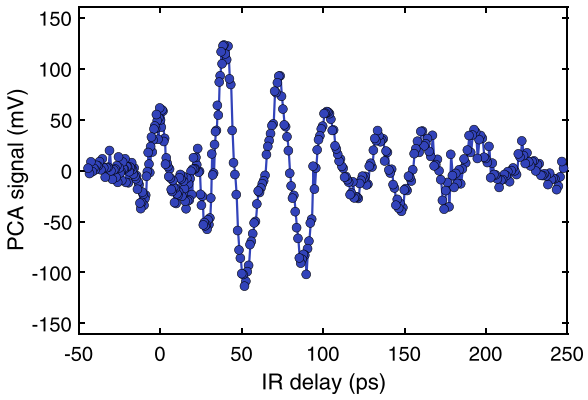

FIG. 3. Timing scan of the PCA signal using a 24 pC electron beam at a distance of about 3.6 mm from the PCA. The observed ringing in the PCA signal is most likely due to multiple reflections within the PCB mount that holds the PCA.

the NIR pulse. At each stage position, this average voltage is collected with beam on and beam off. The scan of the PCA signal as a function of stage delay shown in Fig. 3 plots the average "beam on" shots with the background, determined from average "beam off" shots, subtracted.

A clear time-dependent response is observed and can be used to monitor the relative time-of-arrival between the optically gating NIR pulse and the electron beam. The diagnostic accuracy can be estimated by the ratio of signal noise, σ_V, determined from multiple shots, to the slope of the leading edge, dV/dt. For the measurements in Fig. 3, this value is 0.7 ps. The timing scans show a prolonged ringing at around 34 GHz that begins after the initial signal peak. We believe that this feature is not due to the field of the electron beam, but rather reflections within the printed circuit board (PCB) mount that holds the PCA, because similar ringing in the PCA signal is observed when detecting the transient electric field of a THz pulse produced via optical rectification of the NIR laser (not shown). As we will discuss later, further investigation of this technique should include optimization of the packaging.

In subsequent measurements, we examine the effects of beam charge and distance from the PCA on the signal magnitude, shown in Figs. 4 and 5, respectively. The charge scan in Fig. 4 shows that the detector is sensitive down to very low charge, with noise beginning to obscure the time-dependent signal at around 2 pC. This threshold is consistent with bench-top measurements of a THz pulse generated via optical rectification in which the plasmonics-enhanced PCA was able to easily resolve an electric field magnitude as low as 5 kV/m. These results indicate that a PCA-based timing diagnostic should be suitable for the charge range (a few 100 fC up to 1 pC) typical of sub-picosecond resolution UED experiments.[4,35] Like the timing method demonstrated at UCLA in Ref. 5, this technique is particularly well suited for UED experiments in which the NIR pulse, used to gate photocarriers in the PCA, can also be used for pumping lattice excitations,[36,37] with the added benefit of the non-invasive measurement.

The proof-of-principle measurements presented here demonstrate a promising diagnostic technique, with a clear path towards further optimization. In order to further increase the output signal (and allow measurements of even lower charge beams), the total area of the detector could easily be increased to capture a larger portion of the field generated by the electron bunch. The signal magnitude could also be increased by changing the nanoantenna array geometry to subtend the electron-beam-generated radial field and match the polarization, as already demonstrated for non-plasmonics-enhanced devices.[38–40] Such a detector can offer a larger responsivity by capturing the electron beam field more efficiently than the model designed for linear polarization.

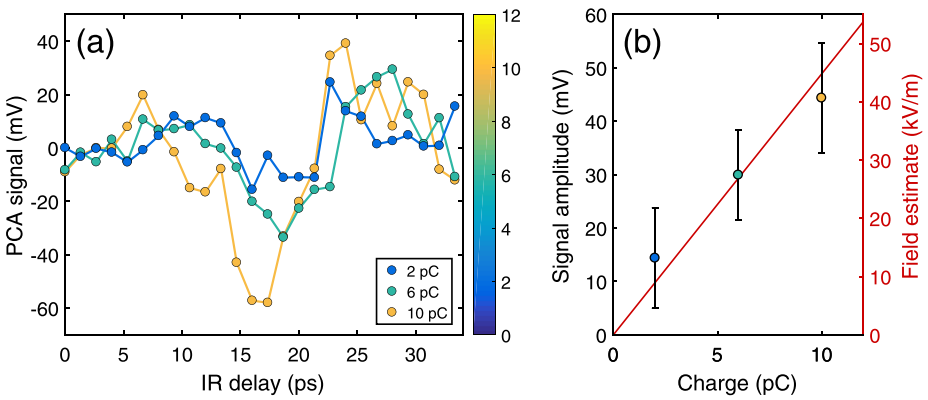

FIG. 4. (a) Timing scans performed using three different beam charges, passing at a distance of 3.6 mm from the PCA. (b) Peak values from these three scans, plotted as a function of the charge, with an analytical prediction for the electric field shown in red.

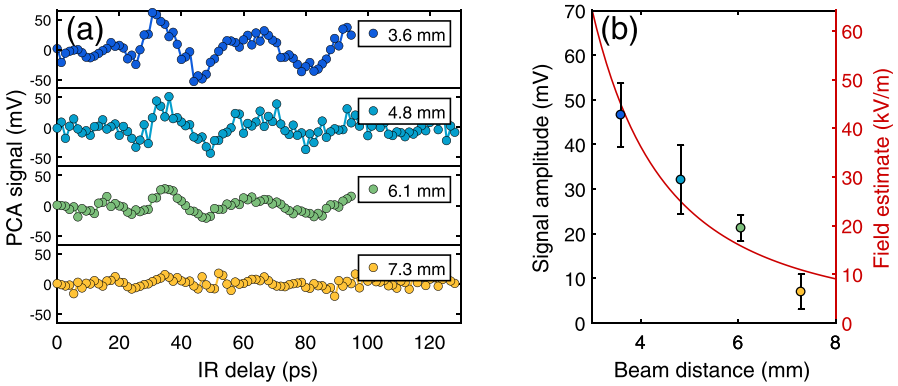

FIG. 5. (a) Timing scans performed using a 10 pC beam passing at different distances from the PCA. (b) Peak values from these four scans, plotted as a function of the distance to the PCA, with an analytical prediction for the field shown in red.

Improvements to the device packaging may also help reduce the noisy background from the RF system driving the accelerator. Simple shielding precautions can be taken to reduce environmental noise, and advanced packaging techniques could potentially reduce or eliminate the ringing on the signal. In future designs, the PCA should be positioned at the very edge of the PCB board, or ideally extending out beyond it, to eliminate any beam obstruction by the board itself.

The temporal resolution of this timing diagnostic is ultimately limited by factors like the pulse width of the NIR beam and the PCA itself. The PCA broadens the pulse due to the relaxation times within the semiconductor. For example, the pulse width of the induced ultrafast photocurrent within a similar PCA was found to be as low as 450 fs FWHM when illuminated by an NIR beam with a pulse width of 135 fs FWHM and a terahertz pulse arriving at normal incidence.[26] With optimizations like improved packaging and NIR alignment, we expect that the temporal resolution in this experimental setup could be smaller than 450 fs, since the pulse width of the NIR beam is <50 fs.

Through these avenues of increasing signal and decreasing noise, the improvement to signal-to-noise ratio can provide even better timing resolution and make this robust detection scheme suitable for a wide range of accelerator applications. Further advances could include an array of discrete antennas with a defocused gating pulse covering the multi-antenna device. A longitudinal configuration would provide a single-shot measurement of the temporal bunch profile, while a transverse arrangement could act as a beam position monitor. The development of this plasmonics-enhanced PCA as an electron beam diagnostic invites a vast range of accelerator applications given the benefits of its simple implementation, robust alignment, small beamline footprint, and the potential for significant improvements in signal resolution.

This work was supported by the Moore Inventor Fellowship, as well as DOE Grant Nos. DE-SC0009914 and NSF Grant PHY-1734215. The authors acknowledge useful discussions with G. Andonian and D. Cesar.

[1]R. K. Li, H. To, G. Andonian, J. Feng, A. Polyakov, C. M. Scoby, K. Thompson, W. Wan, H. A. Padmore, and P. Musumeci, Phys. Rev. Lett. **110**(7), 074801 (2013).
[2]D. Bar-Lev and J. Scheuer, Phys. Rev. Spec. Top.-Accel. Beams **17**(12), 121302 (2014).
[3]P. Musumeci, J. T. Moody, C. M. Scoby, M. S. Gutierrez, M. Westfall, and R. K. Li, J. Appl. Phys. **108**(11), 114513 (2010).
[4]G. Sciaini and R. D. Miller, Rep. Prog. Phys. **74**(9), 096101 (2011).
[5]D. B. Cesar, P. Musumeci, and D. Alesini, J. Appl. Phys. **118**(23), 234506 (2015).
[6]F. Tavella, N. Stojanovic, G. Geloni, and M. Gensch, Nat. Photonics **5**(3), 162 (2011).
[7]M. Harmand, R. Coffee, M. R. Bionta, M. Chollet, D. French, D. Zhu, D. M. Fritz, H. T. Lemke, N. Medvedev, B. Ziaja, and S. Toleikis, Nat. Photonics **7**(3), 215 (2013).
[8]N. Hartmann, H. Wolfram, G. Andreas, M. R. Bionta, J. Grünert, S. L. Molodtsov, K. R. Ferguson, S. Schorb, M. L. Swiggers, S. Carron, and C. Bostedt, Nat. Photonics **8**(9), 706 (2014).
[9]D. J. Gibson, S. G. Anderson, C. P. Barty, S. M. Betts, R. Booth, W. J. Brown, J. K. Crane, R. R. Cross, D. N. Fittinghoff, F. V. Hartemann, and J. Kuba, Phys. Plasmas **11**(5), 2857–2864 (2004).
[10]J. Van Tilborg, C. B. Schroeder, C. V. Filip, C. Tóth, C. G. R. Geddes, G. Fubiani, R. Huber, R. A. Kaindl, E. Esarey, and W. P. Leemans, Phys. Rev. Lett. **96**(1), 111102 (2006).
[11]B. Hidding, J. B. Rosenzweig, Y. Xi, B. O'Shea, G. Andonian, D. Schiller, S. Barber, O. Williams, G. Pretzler, T. Königstein, and F. Kleeschulte, AIP Conf. Proc. **1507**(1), 570–575 (2012).
[12]P. Craievich, S. Di Mitri, M. Milloch, G. Penco, and F. Rossi, Phys. Rev. Spec. Top.-Accel. Beams **16**(9), 090401 (2013).
[13]R. Pompili, M. P. Anania, M. Bellaveglia, A. Biagioni, G. Castorina, E. Chiadroni, A. Cianchi, M. Croia, D. Di Giovenale, M. Ferrario, and F. Filippi, New J. Phys. **18**(8), 083033 (2016).
[14]Z. Zhang, Y. Du, L. Yan, Q. Du, J. Hua, J. Shi, J. Yang, D. Wang, W. Huang, H. Chen, and C. Tang, Phys. Rev. Spec. Top.-Accel. Beams **17**(3), 032803 (2014).
[15]R. K. Li and C. X. Tang, Nucl. Instrum. Methods Phys. Res. Sect. A **605**(3), 243–248 (2009).
[16]A. L. Cavalieri, D. M. Fritz, S. H. Lee, P. H. Bucksbaum, D. A. Reis, J. Rudati, D. M. Mills, P. H. Fuoss, G. B. Stephenson, C. C. Kao, and D. P. Siddons, Phys. Rev. Lett. **94**(11), 114801 (2005).
[17]F. Löhl, V. Arsov, M. Felber, K. Hacker, W. Jalmuzna, B. Lorbeer, F. Ludwig, K. H. Matthiesen, H. Schlarb, B. Schmidt, and P. Schmüser, Phys. Rev. Lett. **104**(14), 144801 (2010).
[18]C. Schmidt, M. K. Bock, S. Pfeiffer, H. Schlarb, W. Koprek, and W. Jalmuzna, in *Proceedings FEL'11* (2011), Vol. 531, p. THPA26.
[19]J. Frisch, in *Proceedings IBIC'15* (2015), p. TUALA01.
[20]A. Angelovski, M. Kuntzsch, M. K. Czwalinna, A. Penirschke, M. Hansli, C. Sydlo, V. Arsov, S. Hunziker, H. Schlarb, M. Gensch, and V. Schlott, Phys. Rev. Spec. Top.-Accel. Beams **18**(1), 012801 (2015).
[21]A. Brachmann, C. Bostedt, J. Bozek, R. Coffee, F. J. Decker, Y. Ding, D. Dowell, P. Emma, J. Frisch, S. Gilevich, and G. Haller, in *Proceedings IPAC'10* (2010), p. TUPE066.
[22]H. Matthias, B. Zeitler, A. Angelovski, S. Vilcins, R. Jakoby, H. Schlarb, K. Floettmann, D. Lipka, A. Penirschke, and F. Grüner, in *Proceedings IPAC'14* (2014), p. TUPRI104.
[23]X. Yan, A. M. MacLeod, W. A. Gillespie, G. M. H. Knippels, D. Oepts, A. F. G. van der Meer, and W. Seidel, Phys. Rev. Lett. **85**(16), 3404 (2000).
[24]C. M. Scoby, P. Musumeci, J. T. Moody, and M. S. Gutierrez, Phys. Rev. Spec. Top.-Accel. Beams **13**(2), 022801 (2010).
[25]N. T. Yardimci, S. H. Yang, C. W. Berry, and M. Jarrahi, IEEE Trans. Terahertz Sci. Technol. **5**(2), 223–229 (2015).
[26]N. T. Yardimci and M. Jarrahi, Sci. Rep. **7**, 42667 (2017).
[27]P. R. Smith, D. H. Auston, and M. C. Nuss, IEEE J. Quantum Electron. **24**(2), 255 (1988).

[28]G. Zhao, R. N. Schouten, N. Van Der Valk, W. T. Wenckebach, and P. C. M. Planken, Rev. Sci. Instrum. **73**(4), 1715 (2002).
[29]P. U. Jepsen, R. H. Jacobsen, and S. R. Keiding, J. Opt. Soc. Am. B **13**(11), 2424 (1996).
[30]K. Kan, I. Nozawa, Y. Yoshida, T. Kondoh, M. Gohdo, and J. Yang, in *Proceedings IPAC'16* (2016), p. MOPMB026.
[31]K. Kan, M. Gohdo, T. Kondoh, I. Nozawa, J. Yang, and Y. Yoshida, in *Proceedings IBIC'16* (2016), p. TUPG58.
[32]C. W. Berry, N. Wang, M. R. Hashemi, M. Unlu, and M. Jarrahi, Nat. Commun. **4**, 1622 (2013).
[33]B. Heshmat, H. Pahlevaninezhad, Y. Pang, M. Masnadi-Shirazi, R. Burton Lewis, T. Tiedje, R. Gordon, and T. E. Darcie, Nano Lett. **12.12**, 6255 (2012).
[34]F. Peter, S. Winnerl, S. Nitsche, A. Dreyhaupt, H. Schneider, and M. Helm, Appl. Phys. Lett. **91**(8), 081109 (2007).
[35]S. P. Weathersby, G. Brown, M. Centurion, T. F. Chase, R. Coffee, J. Corbett, J. P. Eichner, J. C. Frisch, A. R. Fry, M. Gühr, and N. Hartmann, Rev. Sci. Instrum. **86**(7), 073702 (2015).
[36]F. Carbone, P. Musumeci, O. J. Luiten, and C. Hebert, Chem. Phys. **392**(1), 1–9 (2012).
[37]H. C. Shao and A. F. Starace, Phys. Rev. Lett. **105**(26), 263201 (2010).
[38]T. I. Jeon, J. Zhang, and D. Grischkowsky, Appl. Phys. Lett. **86**(16), 161904 (2005).
[39]S. Winnerl, B. Zimmermann, F. Peter, H. Schneider, and M. Helm, Opt. Express **17**(3), 1571–1576 (2009).
[40]S. Winnerl, J. Infrared, Millimeter, Terahertz Waves **33**(4), 431–454 (2012).